Carcinogenesis, 2020, Vol. 41, No. 9, 1219–1228

doi:10.1093/carcin/bgaa072
Advance Access Publication July 6, 2020
Original Article

ORIGINAL ARTICLE

Evaluation of an aldo-keto reductase gene signature with prognostic significance in colon cancer via activation of epithelial to mesenchymal transition and the p70S6K pathway

Seçil Demirkol Canlı[1,†], Esin Gülce Seza[1,†], Ilir Sheraj[1], Ismail Gömçeli[2], Nesrin Turhan[3], Steven Carberry[4], Jochen H.M.Prehn[4], Ali Osmay Güre[5] and Sreeparna Banerjee[1,6,*]

Molecular Pathology Application and Research Center, Hacettepe University, Ankara 06100, Turkey [1]Department of Biological Sciences, Orta Dogu Teknik Universitesi, Ankara 06800, Turkey. [2]Department of Gastroenterological Surgery, Antalya Education and Research Hospital, Antalya 07100, Turkey [3]Department of Pathology, Ankara City Hospital, University of Health Science, Ankara 06800, Turkey [4]Department of Physiology and Medical Physics, Centre for Systems Medicine, Royal College of Surgeons in Ireland, 123 St Stephen's Green, Dublin 2, Ireland [5]Department of Molecular Biology and Genetics, Bilkent University, Ankara 06800, Turkey [6]Cancer Systems Biology Laboratory (CanSyl) Orta Dogu Teknik Universitesi, Ankara 06800, Turkey.

[†]These authors contributed equally to this study.
[*]To whom correspondence should be addressed. Tel: +90 312 210 6468; Fax: +90 312 210 7976; Email: banerjee@metu.edu.tr

Abstract

AKR1B1 and AKR1B10, members of the aldo-keto reductase family of enzymes that participate in the polyol pathway of aldehyde metabolism, are aberrantly expressed in colon cancer. We previously showed that high expression of AKR1B1 ($AKR1B1^{HIGH}$) was associated with enhanced motility, inflammation and poor clinical outcome in colon cancer patients. Using publicly available datasets and *ex vivo* gene expression analysis ($n = 51$, Ankara cohort), we have validated our previous *in silico* finding that $AKR1B1^{HIGH}$ was associated with worse overall survival (OS) compared with patients with low expression of AKR1B1 ($AKR1B1^{LOW}$) samples. A combined signature of $AKR1B1^{HIGH}$ and $AKR1B10^{LOW}$ was significantly associated with worse recurrence-free survival (RFS) in microsatellite stable (MSS) patients and in patients with distal colon tumors as well as a higher mesenchymal signature when compared with $AKR1B1^{LOW}/AKR1B10^{HIGH}$ tumors. When the patients were stratified according to consensus molecular subtypes (CMS), $AKR1B1^{HIGH}/AKR1B10^{LOW}$ samples were primarily classified as CMS4 with predominantly mesenchymal characteristics while $AKR1B1^{LOW}/AKR1B10^{HIGH}$ samples were primarily classified as CMS3 which is associated with metabolic deregulation. Reverse Phase Protein Array carried out using protein samples from the Ankara cohort indicated that $AKR1B1^{HIGH}/AKR1B10^{LOW}$ tumors showed aberrant activation of metabolic pathways. Western blot analysis of $AKR1B1^{HIGH}/AKR1B10^{LOW}$ colon cancer cell lines also suggested aberrant activation of nutrient-sensing pathways. Collectively, our data suggest that the $AKR1B1^{HIGH}/AKR1B10^{LOW}$ signature may be predictive of poor prognosis, aberrant activation of metabolic pathways, and can be considered as a novel biomarker for colon cancer prognostication.

Received: March 17, 2020; **Revised:** June 4, 2020; **Accepted:** July 2, 2020

Abbreviations

AKRs	aldo-keto reductases
CMS	consensus molecular subtypes
COAD	colon adenocarcinoma
DFS	disease-free survival
EMT	epithelial to mesenchymal transition
GLM	general linear model
MSS	microsatellite stable
OS	overall survival
RFS	recurrence-free survival
RPPA	reverse phase protein array

Introduction

In cancer cells, excess glucose can either be metabolized through glycolysis or shunted into the pentose phosphate pathway (1). An additional pathway that becomes active in the presence of excess glucose is the polyol pathway. Aldo-keto reductases (AKRs) are NADPH-dependent enzymes of the polyol pathway that catalyze the reduction of glucose and other carbonyl group containing substrates such as retinals, quinones and lipid peroxidation by-products (2).

Over 150 AKR enzymes belonging to 15 different families have been identified. Although their preferred substrates may vary, these enzymes have a conserved sequence identity and share an $(\alpha/\beta)_8$-barrel fold and an NADPH-binding pocket (2). AKR1B1 and AKR1B10 are two of the best-studied mammalian AKR enzymes that have structural and functional similarities (3). However, unlike the ubiquitous expression of AKR1B1, AKR1B10 is mostly expressed in the colon, small intestine, adrenal glands and liver (4). While AKR1B1 is a rate-limiting enzyme in the conversion of excess glucose to sorbitol, AKR1B10 is a poor reductant of glucose but can reduce retinals and cytotoxic aldehydes (5).

AKRs have been studied for many decades in the context of diabetic complications (6); however, the role of these enzymes in cancer is being increasingly appreciated in recent years (7). We have shown that in colon cancer, AKR1B1 and AKR1B10 have opposing roles; thus, high expression of AKR1B1 was associated with increased proliferation, motility and expression of inflammatory markers, while the opposite was observed with high expression of AKR1B10 (8). Metastasis of cancer cells involves a series of events called the metastatic cascade to travel from the primary tumor to distant metastatic sites and establish secondary tumors (9). Epithelial cells in the primary tumor are thought to undergo epithelial to mesenchymal transition (EMT) to detach from neighboring cells and acquire the ability to migrate independently through the vasculature. This paradigm has recently been refuted in a number of tumor models; the current understanding suggests that EMT may be seen at the primary tumor site thereby enhancing the motility of the cancer cells, while circulating tumor cells that can metastasize to distant organs were shown to have both epithelial and mesenchymal characteristics (10).

The expression of EMT markers is known to be associated with poor clinical outcomes (11). In colorectal cancer, loss of E-cadherin, a major junctional protein and epithelial marker, and increased expression of mesenchymal markers Slug and Vimentin (VIM) were shown to be associated with poor prognosis (12–14). This is due to enhanced metastasis, stemness, therapy resistance and immune evasion in the mesenchymal cells (11).

The expressions of AKR1B1 and AKR1B10 are known to have prognostic significance in different tumor types. AKR1B1 was shown to be strongly associated with an EMT phenotype in lung cancer patients and a rodent model of EMT-driven colon cancer (15). Reduced expression of AKR1B10 in colorectal cancer patients was associated with decreased survival and poor prognosis (16). We have reported that a combination of low expression of AKR1B10 and high expression of AKR1B1 was associated with shorter disease-free survival (DFS) independent of age, gender, *KRAS* or *BRAF* mutations and TNM stage (8).

Using a combination of bioinformatics analysis of publicly available RNA sequencing, microarray and reverse-phase protein array (RPPA) data, as well as confirmatory experiments using *ex vivo* colon and rectal tumor samples and *in vitro* colon cancer cell lines, we report here that high expression of AKR1B1 plus low expression of AKR1B10 ($AKR1B1^{HIGH}/AKR1B10^{LOW}$) was associated with a stronger mesenchymal signature when compared with $AKR1B1^{LOW}/AKR1B10^{HIGH}$ or low/high expression of either gene alone. Mechanistically, this was associated with the aberrant activation of the p70S6K pathway, suggesting that dysregulated metabolic pathways can enhance EMT characteristics, leading to poor prognosis in colorectal cancer patients. We suggest that a combined $AKR1B1^{HIGH}/AKR1B10^{LOW}$ signature can be considered to be a novel biomarker of prognostic value in colorectal cancer.

Materials and methods

Patient characteristics

For *ex vivo* validation, we used tumor tissues obtained from 32 patients with a pathological diagnosis of colon cancer and 19 patients diagnosed with rectal cancer, collected at the Department of Gastroenterological Surgery, Yuksek Ihtisas Training and Research Hospital, Ankara, Turkey, following informed consent obtained from all patients. Information regarding OS time, follow-up status, age, gender, TNM stage, grade, perineural invasion and vascular invasion were available for 46–49 patients. Patient characteristics are shown in Supplementary Table 1, available at *Carcinogenesis* Online. The study was approved by the Bilkent University Ethics Committee.

Analyses of gene expression data

Microarray-based colon tumor expression data [GSE39582 (17), GSE17536 (18) and GSE17537 (19)] were downloaded from GEO (http://www.ncbi.nlm.nih.gov/geo) and RMA normalized using "affy" package from bioconductor. Clinical data related to these samples were downloaded from ArrayExpress (http://www.ebi.ac.uk/arrayexpress). For GSE39582, 566 tumor samples were used in gene expression correlation analyses. Oncotype Dx risk groups were defined for patients based on the expression of 7 genes and 5 reference genes in GSE39582 cohort as previously defined (17). Consensus molecular subtypes (CMS) information for GSE39582 was obtained from www.synapse.org.

Colon Adenocarcinoma (COAD) HTSeq pre-aligned raw read counts for 456 patients (456 tumor and 41 adjacent normal) were downloaded from TCGA data portal by *TCGABiolinks* package (20) in R environment. *DESeq2* package (21) was used for read-count normalization using a general linear model for batch (HiSeq versus GA) and sample status (Tumor versus Normal) (~batch + status). Raw RNA-sequencing read counts for large intestine cell lines (n = 55) were downloaded from CCLE repository and normalized in a similar way by DESeq2 for single factor (~1). Variance-stabilizing transformation expression values for the genes of interest were extracted and used for ranking and correlations. Normalized RPPA data for COAD were downloaded from firebrowse repository (http://firebrowse.org/) of Broad Institute and matched to patients with available RNA sequencing data (n = 358).

Aldo-keto reductase-based subgrouping of CRC tumor samples

Since the prognostic performance of the AKR1B1 and AKR1B10 genes was primarily evaluated in GSE39582, cut-offs with the lowest log-rank P-value

within the interquartile range for the two genes were used to divide 'High' and 'Low' expression groups based on log-rank multiple cut-off analyses as described previously (22). Based on these, samples with "high AKR1B1 and low AKR1B10" (AKR1B1^{HIGH}/AKR1B10^{LOW}), "low AKR1B1 and high AKR1B10" (AKR1B1^{LOW}/AKR1B10^{HIGH}) were assigned. The rest of the samples with "high AKR1B1 and high AKR1B10" and "low AKR1B1 and low AKR1B10" were classified as the "Intermediate" group. The three groups were kept nearly equally sized by using the mean rank difference of expression for AKR1B1 and AKR1B10 in TCGA COAD. Aldo-keto reductase subgroups for GSE17536 dataset and the *ex vivo* cohort were determined with a median expression as cut-offs for both genes due to smaller sample sizes.

EMT-based subgrouping of CRC tumor samples

Tumor samples were classified according to their EMT score based on the expression of E-cadherin (CDH1) and VIM as described previously (23). Briefly, minimum CDH1 and VIM expressions were assigned the scores 0 and –1, while maximum CDH1 and VIM expressions were assigned as –1 and 0, respectively, and the values in between were recalculated between these ranges relative to their original expression values. The sum of the recalculated values generated a CDH1-VIM score with a range between –2 and 0 from the most epithelial to the most mesenchymal. For the categorical analyses, samples with CDH1-VIM score above and below "–1" were considered "mesenchymal" and "epithelial", respectively.

Reverse-phase protein array

Protein extraction from CRC fresh frozen tumors was conducted on dry ice (24) (see Supplementary Table 2, available at *Carcinogenesis* Online, for details). Three parts of cell lysates were mixed with one part SDS buffer [40% glycerol, 8% SDS, 0.25 M Tris–HCl, pH 6.8, plus Bond-Breaker TCEP Solution (Pierce Biotechnology, IL)] at one-tenth of the volume and boiled. Lysates were manually diluted in 4-fold serial dilutions with the SDS buffer. Sample arrays were created on Oncyte Avid nitrocellulose-coated slides (Grace Bio-Labs, OR) by an Aushon 2470 arrayer (Quanterix, Billerica, MA) as per manufacturer's protocol. Immunostaining was performed on an automated slide stainer (AutoLink 48, Dako, CA) according to the manufacturer's instructions (CSA kit, Dako).

Each slide was incubated with a single prevalidated primary antibody (see Supplementary Table 2, available at *Carcinogenesis* Online, for the list of antibodies used) at room temperature for 30 min. Secondary antibodies used were goat anti-rabbit IgG (1:5000) (Vector Laboratories, CA) or rabbit anti-mouse IgG (1:10) (Dako). Detection was with horseradish peroxidase-mediated biotinyl tyramide with chromogenic detection (diaminobenzidine) according to the manufacturer's instructions (Dako).

Scanned TIFF images of slides were analyzed using MicroVigene software V.5.1 (VigeneTech, MA) to generate spot signal intensities (25). The RPPA module of MicroVigene uses a four-parameter logistic-log model ('SuperCurve' algorithm (26)) with all spots within one array employed to form a sigmoid antigen-binding kinetic curve. The protein concentrations were normalized by global sample median normalization.

Cell culture and stable gene expression

The human colon cancer cell line SW480 was cultured in Leibovitz's medium in a humidified atmosphere at 37°C and 100% air. RKO cells cultured in Eagle's minimum essential medium in a humidified atmosphere at 37°C and 5% CO_2. Both cell lines were supplemented with 1% Penicillin Streptomycin, a prophylactic dose of Plasmocin (2.5μg/ml) and 10% fetal bovine serum. SW480 and RKO cells were purchased from ATCC in 2013 and 2014, respectively. The cell lines were authenticated in 2016 at the University of Arizona Genetics Core, USA and in 2020 at Intergen Laboratories, Ankara, Turkey by STR analysis. Both cell lines were routinely tested for mycoplasma contamination by PCR (27).

For the overexpression of AKR1B1 and AKR1B10, the coding sequences were first cloned into a pLenti-Puro transfer vector (a gift from le-Ming Shin (28) Addgene #39481). Viral particles were generated in HEK293FT cells transfected with the cloned transfer vector and psPAX2 and pCMV-VSV-G as the envelope and packaging plasmids, respectively, using Polyethyleneimine (Sigma, Taufikerchen, Germany) at a ratio of 1:3 for DNA: Polyethyleneimine. The supernatant was filtered through 0.45 μm PES syringe filters. Infection of colon cancer cell lines was carried out at a ratio of 1:1 of supernatant and cell culture medium supplemented with polybrene (1:1000, v/v) to enhance infection efficiency. Seventy-two hours after infection, polyclones were selected with 1 μg/ml puromycin and overexpression was confirmed by Western blot and PCR. Selection pressure was continued with a maintenance dose of puromycin (0.5 μg/ml).

Western blot

Total proteins from the AKR1B1 and AKR1B10 overexpressing RKO and SW480 cell lines were extracted using the MPER Mammalian Protein Extraction Buffer (Thermo Scientific) containing protease and phosphatase inhibitors (Roche). Proteins (20–50μg) were separated in 10% SDS–PAGE gels and transferred to PVDF membranes (polyvinylidene fluoride, Roche) using standard techniques. The antibodies used are shown in Supplementary Table 3A, available at *Carcinogenesis* Online. Bands were visualized with the Clarity ECL Substrate (Bio-Rad, Hercules, CA) and ChemiDoc MP Imaging System (Bio-Rad).

RNA isolation and PCR

Total RNA was extracted from frozen tumor tissue (samples are the same ones used for RPPA) using Trizol reagent (Ambion, Foster City, CA) and from the colon cancer cell lines by using NucleoSpin RNA kit (Macherey Nagel, Düren, Germany) according to the manufacturer's guidelines. The DNAse I (Thermo Scientific)-treated RNA samples (500 ng) were converted to cDNA using a RevertAid First Strand cDNA Synthesis Kit (Thermo Scientific). RT-qPCR reactions were carried out in a CFX Connect (Bio-Rad, Hercules) using standard techniques. Fold changes were calculated with respect to the geometric mean of two internal controls (ACTB and GAPDH) using the Pfaffl method (29). In addition, to account for batch differences in amplification between the different PCR runs using the patient samples as template, cDNA from the epithelial breast carcinoma cell line BT-20 was included in every 96-well PCR plate. The BT-20 cell line was selected as the Ct (cycle threshold) values for all six genes amplified (AKR1B1, AKR1B10, E-cadherin, VIM, GAPDH and ACTB) were found to be below 33. The expression data for each of the genes in the patient samples were normalized to the expression of the same gene in BT-20. The BT-20 expression data were not used for statistical analysis. The primer sequences are shown in Supplementary Table 3B, available at *Carcinogenesis* Online.

Statistical analyses

GraphPad Prism 6.1 (GraphPad Software Inc.), SPSS Statistics v.19 (IBM, 2010, Chicago, IL) or R Language (v.3.6.3) was used for data analysis. Pearson correlation analyses were performed to test linear relationships. Kaplan–Meier plots and the log-rank test were utilized to assess survival differences among groups. Samples with RFS value "0" were excluded from survival analyses. Univariate and multivariate Cox proportional hazards regression analyses were performed using SPSS Statistics v.19. *P*-value of <0.05 was considered statistically significant for all comparisons.

Results

High AKR1B1 and low AKR1B10 expression is associated with poor prognosis

We previously reported that patients with AKR1B1^{HIGH}/AKR1B10^{LOW} tumors had poor prognosis independent of age, gender, KRAS or BRAF mutations and TNM stage versus those with AKR1B1^{LOW}/AKR1B10^{HIGH} tumors (8), which we confirmed in this study using an independent cohort (Figure 1A, Supplementary Table 4, available at *Carcinogenesis* Online). The AKR-signature (AKR-S) could identify significantly distinct prognostic subgroups among MSS or distal tumors (Supplementary Figure 1A–D, available at *Carcinogenesis* Online). A good stratification could be obtained in proximal tumors, especially when they were of an MSS genotype (Supplementary Figure 1E, F, available at *Carcinogenesis* Online). We next examined by RT-qPCR whether the expressions of AKR1B1 and AKR1B10 were of prognostic significance in fresh frozen primary tumors from 32 patients with colon cancer and

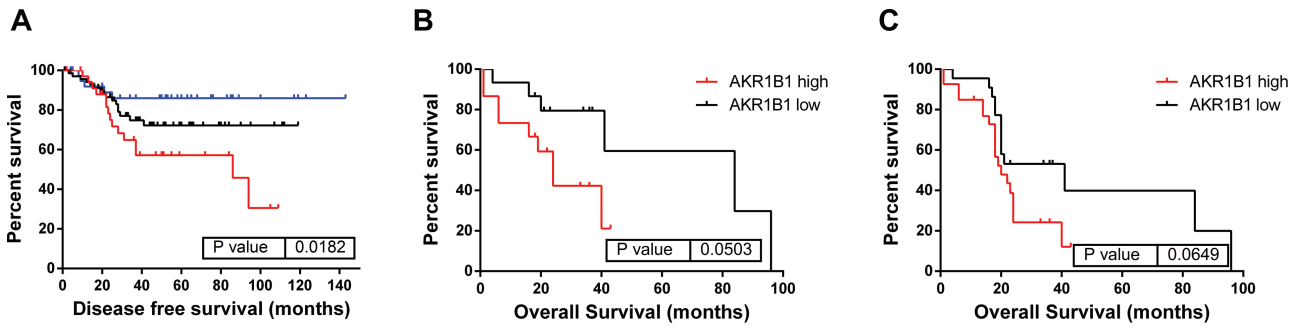

Figure 1. AKR signature is associated with prognosis in colon cancer. Kaplan–Meier plots comparing AKR signature-based groups in GSE17536 (**A**), AKR1B1 expression-based groups in colon tumors (**B**) and colorectal tumors (**C**) of the *ex vivo* Ankara cohort. For Figure 1A, the blue line corresponds to AKR1B1^{LOW}/AKR1B10^{HIGH} samples, the black line corresponds to intermediate and the red line corresponds to AKR1B1^{HIGH}/AKR1B10^{LOW} samples. The expression cut-off for AKR1B1 was determined by log-rank multiple cut-off analyses (see Methods). Log-rank *P*-values are indicated.

19 patients with rectal cancer (Ankara cohort; for patient characteristics see Supplementary Table 1, available at *Carcinogenesis* Online). Colon cancer patients were stratified using cut-off values within the interquartile range of gene expression that gave the highest significance by log-rank multiple cut-off analyses), as described previously (22). We observed that high AKR1B1 expression was associated with a shorter OS with borderline significance in colon and colorectal cancer patients; log-rank $P = 0.0503$ and 0.065, respectively (Figure 1B, C). However, the same comparisons for AKR1B10 high samples did not show any statistical differences; therefore, the AKR-S was not evaluated in this cohort. The prognostic power of AKR1B10 is less when compared with AKR1B1 (8); therefore, a good stratification is more unlikely to be observed in small cohorts. The fact that AKR-S was significantly associated with RFS in GSE39582 (Supplementary Figure 1, Supplementary Table 5, available at *Carcinogenesis* Online) and DFS in GSE17536 (Figure 1A, Supplementary Table 4, available at *Carcinogenesis* Online), but not with OS in the *ex vivo* cohort and disease-specific survival in GSE17536 (data not shown), suggests clearly that AKR-S is related more to disease relapse or aggressiveness rather than the time to death.

We next compared AKR-S with Oncotype Dx, which was developed to predict recurrence in colon cancer for stages II and III patients (30), and can be approximated on microarray-based expression in tumors (17). Both signatures, when evaluated separately, could stratify stages II and III colon cancer patients in GSE39582 (22) (AKR-S: Cox p:0.02, HR:1.327). A multivariate analysis that included both Oncotype Dx risk groups and AKR-S in the model for stages II and III patients showed no significance for either classifications, indicating that the patient groups identified by both signatures overlapped significantly (Supplementary Table 5A available at *Carcinogenesis* Online). However, when stages II and III patients with an MSS genotype were analyzed in a similar manner, AKR-S generated significantly distinct subgroups, whereas Oncotype Dx did not, suggesting that AKR-S was superior in this patient group (Supplementary Table 5B available at *Carcinogenesis* Online). As evident in Kaplan–Meier curves, the Oncotype Dx low-risk group but not high-risk group could be further stratified by the AKR-S, suggesting that this signature could define the prognostic variations in Oncotype Dx-low-risk group (Supplementary Figure 2 available at *Carcinogenesis* Online).

AKR-S is associated with EMT markers

We previously showed that ectopic expression of AKR1B1, but not AKR1B10 was associated with increased motility and weaker cell–cell adhesion in colon cancer cell lines (8). To evaluate whether this was physiologically relevant, we explored an *in silico* correlation between the expression of AKR1B1 and EMT markers in the GSE39582 and TCGA COAD datasets. We observed a strong positive and significant correlation between the expression of AKR1B1 and the mesenchymal markers VIM, ZEB1, ZEB2, TWIST1 and TWIST2 and a significant negative correlation between AKR1B1 and the epithelial marker E-cadherin (CDH1) in both datasets (Supplementary Figure 3A, C, available at *Carcinogenesis* Online). Additionally, a negative correlation was observed between AKR1B10 and the mesenchymal markers indicated above, along a weak but statistically significant positive correlation between AKR1B10 and CDH1 in both datasets (Supplementary Figure 3B, D, available at *Carcinogenesis* Online). Similar correlations were observed between the expression of VIM, CDH1, AKR1B1 and AKR1B10 in the Ankara cohort as determined by RT-qPCR (Supplementary Figure 3E, available at *Carcinogenesis* Online).

A significant positive correlation ($r = 0.604$, $P < 0.00001$) between the expression of AKR1B1 and the EMT score (see Methods) indicated that a higher expression of AKR1B1 was associated with a mesenchymal phenotype (Figure 2A). On the contrary, AKR1B10 expression showed a negative correlation with the EMT score ($r = -0.214$, $P < 0.00001$), indicating that high AKR1B10 expression was associated with a more epithelial phenotype (Figure 2B). Corroborating the *in silico* data, we observed that the EMT score of patients in the Ankara cohort was positively correlated with AKR1B1 expression and negatively correlated with AKR1B10 expression confirming more mesenchymal and epithelial phenotype for patients with high AKR1B1 and high AKR1B10 expression, respectively (Figure 2C, D).

When we analyzed the protein expression of EMT markers from RPPA data available for the TCGA cohort, we observed that the AKR1B1^{HIGH}/AKR1B10^{LOW} samples expressed significantly lower E-cadherin (CDH1) and Claudin 7 (CLDN7) (epithelial markers) and significantly higher Fibronectin (FN1) and Collagen-VI (COL6A1) (mesenchymal markers) when compared with the AKR1B1^{LOW}/AKR1B10^{HIGH} and the intermediate samples (Figure 2E). Data for the protein expression of VIM was not available in the COAD RPPA. These data further corroborate that tumors expressing high levels of AKR1B1 have a more mesenchymal phenotype while tumors expressing high levels of AKR1B10 have an epithelial phenotype.

Next, we asked whether epithelial or mesenchymal phenotype of the tumors could contribute further to prognostic prediction of AKR genes. We first stratified patients based on AKR gene groups and then compared the prognosis of "epithelial" and "mesenchymal" samples defined by EMT score within each

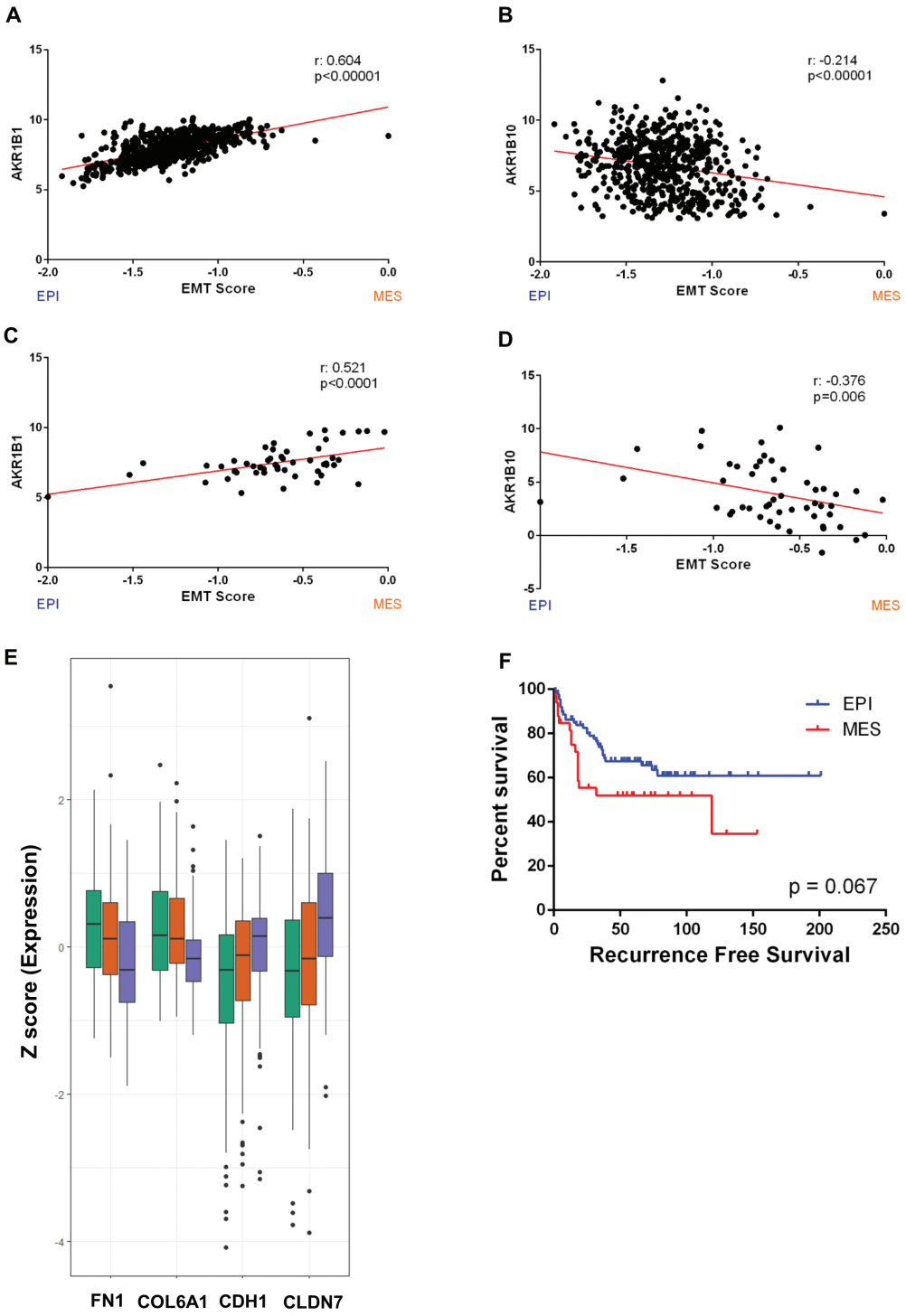

Figure 2. EMT score is related to AKR gene expression. Linear correlation of log expression and EMT score are shown in GSE39582 (**A**, **B**) and *ex vivo* cohort (**C**, **D**). Pearson *r* and *P* values are indicated. (**E**) Box plots for RPPA-based expression of EMT-related genes FN1, COL6A1, CDH1 and CLDN7 in TCGA COAD dataset (n = 358); Colors indicate the AKR groups: green corresponds to AKR1B1^{HIGH}/AKR1B10^{LOW}, orange corresponds to Intermediate and purple corresponds to AKR1B1^{LOW}/AKR1B10^{HIGH}. The groups were compared with one-way ANOVA; *P* <0.00001 for all comparisons (**F**) Kaplan–Meier curve for EPI and MES subgroups in AKR1B1^{HIGH}/AKR1B10^{LOW} patients in GSE39582. Log-rank *P* value is shown.

subgroup in GSE39582. Of note, all AKR1B1^{LOW}/AKR1B10^{HIGH} samples had an epithelial phenotype. However, the AKR1B1^{HIGH}/AKR1B10^{LOW} samples could be classified into epithelial and mesenchymal subgroups (71% epithelial, 29% mesenchymal). AKR1B1^{HIGH}/AKR1B10^{LOW} patients who had a more mesenchymal phenotype showed a relatively shorter RFS compared with AKR1B1^{HIGH}/AKR1B10^{LOW} patients who had a more epithelial phenotype (*P* = 0.067) (Figure 2F). Overall, these findings indicate that unlike the AKR1B1^{HIGH}/AKR1B10^{LOW} samples, the AKR1B1^{LOW}/AKR1B10^{HIGH} samples are relatively homogeneous in terms of their EMT phenotype. Multivariate analyses including AKR-based groups and EMT groups in the model showed that

AKR gene groups and EMT score are independent prognostic predictors (HR: 1.27, $P = 0.04$ and HR: 1.62, $P = 0.04$, respectively).

To evaluate whether the mesenchymal phenotype observed in the AKR1B1^{HIGH}/AKR1B10^{LOW} samples was contributed by the stromal compartment of the tumors, we evaluated whether AKR1B1 expression was correlated with EMT in samples with various levels of stromal involvement. For this, we used a publicly available stromal score from MD Anderson Cancer Center for the COAD RNA-Seq samples used in our study (https://bioinformatics.mdanderson.org/estimate/index.html). Using patient IDs, we matched those patients for whom the stromal score and expression of the genes of interest in the current study were available. We next classified the patients according to low, intermediate and high stromal scores ($n = 44$ for each group) and carried out Pearson correlation analyses between the expression of AKR1B1 and EMT score, and the expression of ZEB1, ZEB2, SNAI1, SNAI2, TWIST1 and TWIST2 in each group separately. We observed that the expression of AKR1B1 was positively correlated with the EMT score with borderline significance in the low stroma group and significantly correlated in the intermediate group; however, the significance was clearly lost in samples with high stroma. Furthermore, several mesenchymal markers ZEB1, ZEB2 and SNAI2 showed a significant correlation only in the low stromal score samples (Supplementary Table 6 available at *Carcinogenesis* Online). The only correlation that reached statistical significance in the high stromal score samples was between the expression of AKR1B1 and TWIST2. These data suggest the lack of a significant linear relationship between AKR1B1 expression and mesenchymal features in tumors with high stroma, indicating that AKR1B1 expression–EMT relationship in CRC tumors is primarily originating from epithelial cells, rather than the stroma.

Categorization of AKR1B1 and AKR1B10 expression into a consensus molecular subtype

When the distribution of AKR1B1^{HIGH}/AKR1B10^{LOW}, intermediate and AKR1B1^{LOW}/AKR1B10^{HIGH} samples among the CMS (31) groups was evaluated, the most striking differences could be seen in CMS3 and CMS4 categories (Table 1). The CMS3 category is characterized by enrichment of genes that are involved in the metabolism of glucose, pentoses, mannose, fructose, galactose, glutamine, glutathione and fatty acids (31). The CMS4 category is characterized by an enrichment of genes associated with EMT activation, TGFβ signaling and a mesenchymal phenotype (31).

We then examined the differential expression of genes in the AKR1B1^{LOW}/AKR1B10^{HIGH} patients from GSE39582 categorized as CMS3 ($n = 46$) and the AKR1B1^{HIGH}/AKR1B10^{LOW} categorized as CMS4 ($n = 62$). When the differentially expressed genes (FDR < 0.05, LFC > abs (0.5)) were analyzed for enrichment of Gene Ontology terms by ClusterProfiler package (32), as expected, metabolic pathways were highly enriched in the patients categorized as CMS3 (AKR1B1^{LOW}/AKR1B10^{HIGH}), whereas pathways related to cellular adhesion and migration in the patients classified as CMS4 (AKR1B1^{HIGH}/AKR1B10^{LOW}) (Supplementary Figure 4 available at *Carcinogenesis* Online).

Altered metabolic signaling pathways are associated with AKR gene expression

It is well established that AKRs are functional in the enzymatic reduction of glucose and other aldehyde substrates, many of which are crucial in metabolism-related pathways. Therefore, we hypothesized that the prognostic value of the AKR-S could stem from the activation of metabolic pathways. To better evaluate this, a custom RPPA consisting of 58 antibodies was generated for our samples. Sixty per cent of the antibodies in this array belongs to the proteins coded by the genes in the "PI3K-Akt signaling pathway" (hsa04151) according to Kyoto Encyclopedia of Genes and Genomes database that are closely involved in glucose metabolism (33). Protein lysates from fresh frozen tissue specimens from the Ankara cohort ($n = 31$, colon cancer only) were used for the RPPA. We observed that the phosphorylation of AKT, mTOR, p70S6K, GSK3β and S6 were in the opposite directions in the AKR1B1^{HIGH}/AKR1B10^{LOW} patients compared with the AKR1B1^{LOW}/AKR1B10^{HIGH} patients (Figure 3A). Since the phosphorylation of GSK3β in the AKR1B1^{HIGH}/AKR1B10^{LOW} patients was significantly lower ($P = 0.007$) than the AKR1B1^{LOW}/AKR1B10^{HIGH} patients, we determined the correlation between GSK3β phosphorylation and other proteins in the AKT pathway. We observed a strong tendency for activation in the opposite direction between samples according to the AKR-S (Figure 3B), suggesting that the entire pathway in this patient cohort was deregulated, most likely based on the difference in GSK3β activation.

We determined the phosphorylation of the same proteins from the RPPA data of COAD samples ($n = 358$) available in TCGA. For these samples, the opposite tendency in the activation of the AKT pathway proteins based on the AKR-S was conserved. However, we observed a statistically significant ($P = 0.016$) but opposite trend in the phosphorylation of GSK3β at S9 when compared with the Ankara cohort (Figure 3C). Additionally, the phosphorylation of p70S6K (T389) was observed to be significantly higher ($P = 0.047$) in the AKR1B1^{HIGH}/AKR1B10^{LOW} samples when compared with the AKR1B1^{LOW}/AKR1B10^{HIGH} samples. Among the downstream targets of p70S6K are S6, a ribosomal protein that is involved in protein translation and PDCD4 that inhibits the initiation of protein translation (34). Although the phosphorylation of S6 at two sites (S240/244 and S235/236) did not change based on the AKR signature, a tendency for increased protein level of PDCD4 was found in the AKR1B1^{LOW}/AKR1B10^{HIGH} samples, which also showed reduced phosphorylation of p70S6K (T389). Next, RPPA of large intestine cell lines ($n = 55$) available in the Cancer Cell Line Encyclopedia (CCLE) (35) was examined for alterations in the activation of the AKT pathway based on the AKR signature (Figure 3D). The only protein whose phosphorylation was significantly altered based on the AKR signature was p70S6K (T389) ($P = 0.0097$) whereby, matching the COAD-RPPA data, higher phosphorylation was observed in the AKR1B1^{HIGH}/AKR1B10^{LOW} samples when compared with the AKR1B1^{LOW}/

Table 1. Distribution of patients in GSE39582 stratified according to the AKR signature in the CMS

Categories	CMS1	CMS2	CMS3	CMS4
AKR1B1^{HIGH}/AKR1B10^{LOW}	23 (16.9%)	47 (34.6%)	**4 (2.9%)**	**62 (45.6%)**
Intermediate	48 (19.8%)	119 (49.2%)	16 (6.6%)	59 (24.4%)
AKR1B1^{LOW}/AKR1B10^{HIGH}	18 (13.5%)	64 (48.1%)	**46 (34.6%)**	**5 (3.8%)**

The chi-square statistic is 120.511, $P < 0.00001$. Values in bold show that the most striking difference in distribution of patients was seen in the CMS3 and CMS4 categories.

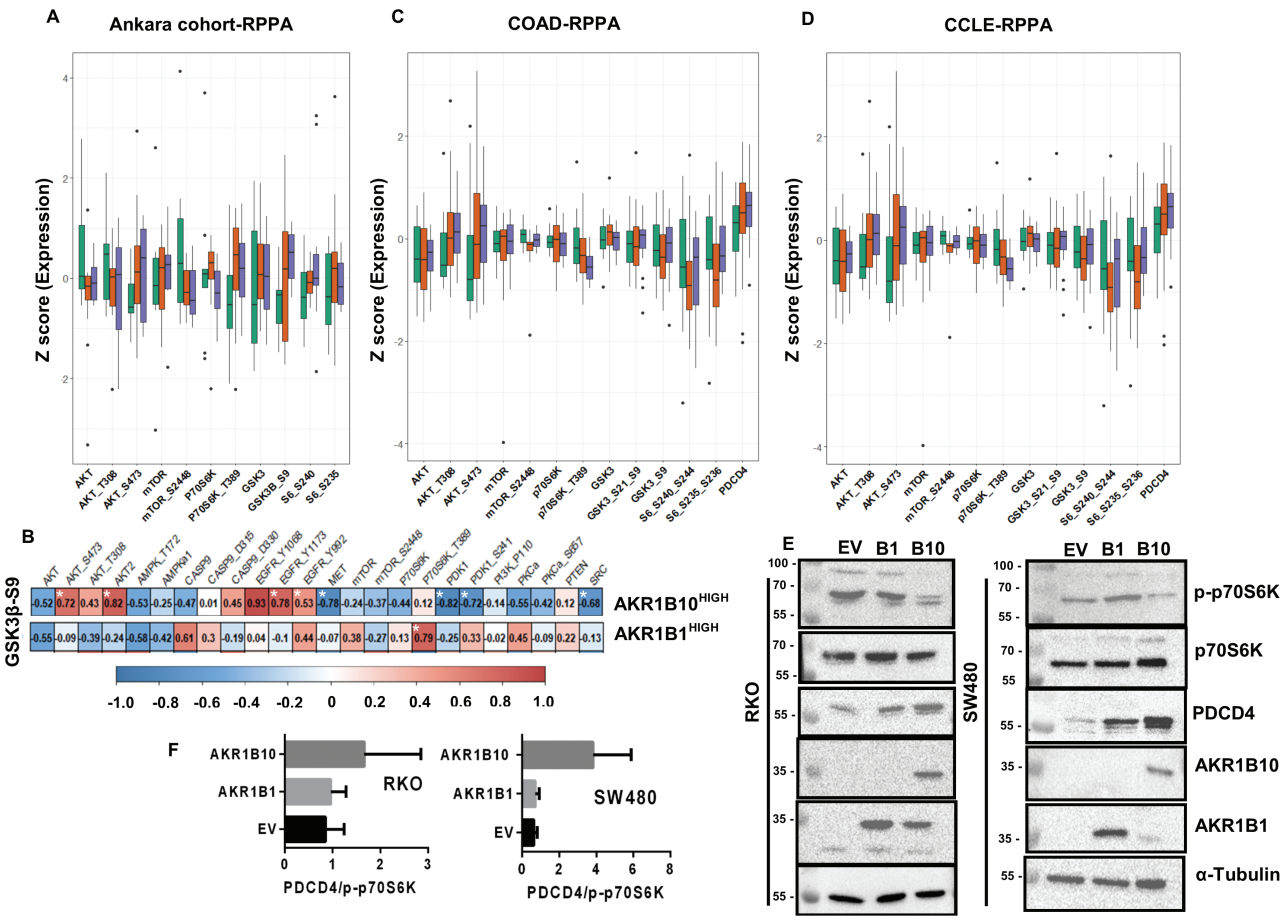

Figure 3. AKR signature is associated with the activation of metabolic pathways. (**A**) RPPA carried out with the Ankara cohort (n = 31, colon cancer only) showed an opposite trend in the activation or expression of several proteins of the AKT pathway based on the AKR signature (AKR-S). A statistically significant increase in the phosphorylation of GSK3β was seen in the AKR1B1^{LOW}/AKR1B10^{HIGH} samples. (**B**) Correlations (Spearman) between the phosphorylated GSK3β and other proteins of the AKT pathway showed in opposite trend according to the AKR-S. Statistically significant correlations are shown with a star. Box plots of the RPPA data in TCGA COAD (n = 358) (**C**) and CCLE (n = 55) (**D**) according to the AKR-S. A decrease in the phosphorylation of p70S6K and an increase in protein levels of PDCD4 were seen in the AKR1B1^{LOW}/AKR1B10^{HIGH} samples. For all bar diagrams, green bars correspond to AKR1B1^{HIGH}/AKR1B10^{LOW}, orange bars correspond to Intermediate and purple bars correspond to AKR1B1^{LOW}/AKR1B10^{HIGH} samples. One-way ANOVA was performed for the comparison of mean protein expression between the AKR groups for RPPA data of TCGA COAD and CCLE, Kruskal–Wallis was performed for comparisons in *ex vivo* RPPA data using SPSS Statistics v.19 (**E**) Western blot showing a significant decrease in the phosphorylation of p70S6K and increase in protein expression of PDCD4 in RKO and SW480 cells overexpressing AKR1B10. All western blot experiments were repeated three times independently with different passages of the stably expressing cells. (**F**) The ratio of western blot band intensity of PDCD4 and p-p70S6K in AKR1B1 and AKR1B10 overexpressing RKO and SW480 cell lines.

AKR1B10^{HIGH} samples. Again, matching the COAD-RPPA data, no alterations were observed in the phosphorylation of S6, but a tendency for the increased protein levels of PDCD4 was found in the AKR1B1^{LOW}/AKR1B10^{HIGH} samples (P = 0.1414).

To further confirm these data, colon cancer cell line models were investigated. SW480 and RKO cells do not express either AKR1B1 or AKR1B10 (8). Therefore, cells overexpressing AKR1B1 were expected to mimic the AKR1B1^{HIGH}/AKR1B10^{LOW} samples while cells overexpressing AKR1B10 were expected to mimic the AKR1B1^{LOW}/AKR1B10^{HIGH} samples. Western blot analyses indicated that the phosphorylation of AKT (T308), mTOR or GSK3β (S9) did not change between in the AKR1B1 or AKR1B10 overexpressing RKO cells, while an increase in p-mTOR (S2481) was seen in SW480 cells (Supplementary Figure 5A, B, available at *Carcinogenesis* Online). However, there was no accompanying increase in the p-AKT. Despite no alterations in the activation of AKT proteins, the RKO cells were not rapamycin resistant as confirmed with a loss in the phosphorylation of mTOR and p70S6K in rapamycin-treated cells (Supplementary Figure 5C available at *Carcinogenesis* Online). On the other hand, a significant decrease in the phosphorylation of p70S6K (T389) was observed in the cell lines overexpressing AKR1B10, (Figure 3E). Supporting the RPPA data from COAD and large intestine CCLE, we observed no alterations in the phosphorylation of S6 (S240/244 and S235/236); however, an increase in the protein levels of PDCD4 was observed in both cell lines overexpressing AKR1B10 (Figure 3E). The PDCD4/p-p70S6K ratio of western blot band intensities suggested that AKR1B10 overexpressing cell lines showed a greater increase in PDCD4 and decrease in p-p70S6K than AKR1B1 overexpressing cells (Figure 3F). Interestingly, the increase in PDCD4 was also seen at the mRNA level in RKO (but not SW480) cells overexpressing AKR1B10 suggesting both transcriptional and post-transcriptional regulation of PDCD4 in RKO cells (Supplementary Figure 5D available at *Carcinogenesis* Online).

Discussion

Colon cancer is characterized by a tight regulation in differentiation, tumor invasion and adjacent organ involvement, and a remarkable worsening of prognosis between late and early

stages of disease (36). Nonetheless, routine clinical practice in colon cancer does not include evaluation of a gene expression signature (37). The identification of molecular prognostic markers can predict patient outcome and benefit treatment decisions on an individual basis. In the current study, we have used multiple patient cohorts in *in silico*, *ex vivo*, cell line and pathway analyses to establish a molecular signature based on the combined expression of AKR1B1 and AKR1B10. AKR1B1^{HIGH}/AKR1B10^{LOW} patients had significantly poor DFS and RFS. These data support a recent four gene signature that included AKR1B10 and was shown to predict better OS in colorectal cancer patients (38). The AKR-S (AKR1B1^{HIGH}/AKR1B10^{LOW}), however, could significantly separate prognostic groups further in the *in silico* adapted version of Oncotype DX colon in Oncotype low-risk stages II and III patients. It is already well established that microsatellite instability is an independent prognostic predictor of better survival and longer RFS (39). When patients were stratified according to microsatellite stability, the AKR1B1^{HIGH}/AKR1B10^{LOW} signature could predict worse RFS in patients with MSS tumors irrespective of the location of the tumor. Thus, the AKR-S may be beneficial in prognostication of MSS tumors. When tumor location was used as strata, the AKR-S could better prognosticate tumors in the distal location. In our *ex vivo* cohort, we could confirm that high expression of AKR1B1 was associated with reduced OS at a borderline significance, but AKR1B10 did not show a relationship. This suggests that the AKR-S is more indicative of RFS and DFS, rather than OS.

A transcriptome analysis of the NCI60 panel and CCLE showed that the expression of AKR1B1 but not AKR1B10 was higher in mesenchymal cell lines (15). Supporting this, we have established that the AKR1B1^{HIGH}/AKR1B10^{LOW} samples primarily conformed to a CMS4 (mesenchymal) phenotype but were relatively heterogeneous and could be further sub-classified into epithelial and mesenchymal categories. Patients belonging to the mesenchymal subgroup showed worse RFS compared with the patients belong to the epithelial subgroup, suggesting that poor prognosis in the AKR1B1^{HIGH}/AKR1B10^{LOW} patients was mostly driven by the mesenchymal characteristics of the tumor.

Gene set enrichment analysis carried out with AKR1B10 high/low samples in GSE39582 indicated a statistically significant enrichment of metabolism-associated pathways in the AKR1B10 high samples; no significant enrichment was seen in the AKR1B10 low samples (data not shown). Additionally, the AKR1B1^{LOW}/AKR1B10^{HIGH} samples in GSE39582 mostly belonged to the CMS3 (metabolic) category. *In silico* analysis of RPPA data from TCGA COAD and CCLE, as well as western blot data from colon cancer cell lines indicated a consistent reduction in the phosphorylation of p70S6K at T389 in the AKR1B1^{LOW}/AKR1B10^{HIGH} samples. p70S6K is known to be a direct target of mTOR and can phosphorylate several proteins involved in protein synthesis, cell growth proliferation and motility (40); the latter via the upregulation of Snail, leading to the repression of E-cadherin (41). Surprisingly, we did not observe any alteration in the phosphorylation of mTOR (S2481); therefore, we speculate that rather than an inhibition of mTOR activity, enhanced dephosphorylation of p70S6K via PP2A like phosphatases could have occurred (42). p70S6K is known to phosphorylate PDCD4 at S67, leading to its proteasomal degradation (43). We observed a significant increase in the protein levels of PDCD4 in the AKR1B1^{LOW}/AKR1B10^{HIGH} samples, most likely due to the reduced kinase activity of p70S6K. PDCD4 is a tumor suppressor that was reported to be associated with a good prognosis in colorectal cancer (44). Additionally, RKO cells overexpressing PDCD4 were reported to exhibit reduced migration via the inhibition of urokinase receptor (45). PDCD4 can also be regulated post-transcriptionally via miR-21; the AKR inhibitor Fidarestat was shown to increase the expression of PDCD4 via downregulation of miR-21 (46). These data suggest that PDCD4 may be an important target to mediate alterations in cellular characteristics observed with high expression of AKR1B10.

RPPA carried out with protein samples isolated from the Ankara cohort indicated that the AKR1B1^{LOW}/AKR1B10^{HIGH} samples showed a remarkable increase in the phosphorylation of GSK3β (S9) and AKT (S473) compared with the AKR1B1^{HIGH}/AKR1B10^{LOW} samples. GSK3β is a highly promiscuous kinase with over 100 substrates (47) and can be phosphorylated at S9 (leading to its inhibition) by several kinases including AKT, protein kinase A, PKC and p70S6K. Of these, AKT-mediated phosphorylation of GSK3β (S9) via insulin receptor signaling is known to carry out an inhibitory phosphorylation of IRS-1 (48). Keeping in mind that AKRs are strongly implicated in the metabolism of excess glucose into polyols in diabetes (49), the activation of an inhibitory pathway for insulin receptor signaling in the presence of high levels of AKRs suggests that these enzymes may even be functional in the development of insulin resistance in colon cancer. Of note, the increased phosphorylation of GSK3β in the AKR1B1^{LOW}/AKR1B10^{HIGH} samples was not observed in the RPPA of COAD or CCLE large intestinal cell lines, or in colon cancer cell lines overexpressing AKR1B10. This may be because the phosphorylation of GSK3β is oscillatory, which may influence the level of phosphorylation observed in the different sample sets (47). Additionally, the Ankara cohort consisted primarily of stage III patients, which may have influenced the signal transduction pathways activated. Cancer cachexia is an incurable debilitating comorbidity of cancer that has no treatment options and is associated with poor outcomes (50). Increased phosphorylation of AKT (S473) is associated with enhanced protein synthesis and muscle growth through de-repression of the mTOR signaling (51). Although the patient sample used in the current study did not have any data on cancer cachexia, we speculate that one of the outcomes of increased AKT phosphorylation in the AKR1B1^{LOW}/AKR1B10^{HIGH} patients could be an amelioration of cachexia, leading to a better prognosis.

Overall, we have shown here that an AKR1B1^{HIGH}/AKR1B10^{LOW} gene signature could act as an independent prognostic factor for poor RFS and DFS while the AKR1B1^{LOW}/AKR1B10^{HIGH} signature was associated with good RFS and DFS in independent patient cohorts, particularly with MSS and distal tumors. Expression of AKR1B1, but not AKR1B10 was also found to be higher in the poor prognosis group *ex vivo*, when OS was used as the clinical outcome. Mechanistically, we have shown that the AKR1B1^{HIGH}/AKR1B10^{LOW} signature was associated with enhanced mesenchymal properties while the AKR1B1^{LOW}/AKR1B10^{HIGH} signature was primarily epithelial and characterized by the inhibition of metabolic pathways associated with biomass production and cell proliferation. Further validation of this gene expression signature, especially in prospective cohorts and better mechanistic characterization of AKR1B1^{HIGH}/AKR1B10^{LOW} tumors are needed to evaluate these enzymes as drug targets. The AKR inhibitor Epalrestat has been FDA approved for the treatment of diabetic complications, but its selectivity for the different AKR isoforms and efficacy in colorectal cancer are unknown (52). Opportunities for the design of selective AKR1B1 inhibitors that do not target AKR1B10 will be of interest in the future.

Supplementary material

Supplementary data are available at *Carcinogenesis* online.

Funding

The study was funded by the Scientific and Technological Research Council of Turkey (TÜBİTAK) as a part of the COST action CA17118, grant no 118Z688 to SB, YÖK 100/2000 bursary to EGS and Science Foundation Ireland and Health Research Board Investigator Award 14/IA/2582; 16/US/3301 to JHMP.

Acknowledgments

The authors gratefully acknowledge Ismail Guderer for generating the AKR1B1 and AKR1B10 overexpressing cell lines used in this study, Dr. Sahika Cingir Koker (Ufuk University, Ankara), Dr. Onur Cizmecioglu (Bilkent University, Ankara), Dr. Elif Erson-Bensan and Dr. Rengul Cetin Atalay (Middle East Technical University, Ankara) for sharing resources and ideas. The vector psPAX2 was a gift from Didier Trono (Addgene plasmid #12260; http://n2t.net/addgene:12260; RRID:Addgene_12260) and the vector pCMV-VSV-G was a gift from Bob Weinberg, (Addgene plasmid #8454; http://n2t.net/addgene:8454; RRID:Addgene_8454).

Conflict of Interest Statement: The authors declare that they have no financial or non-financial conflicts of interest.

References

1. Hamanaka, R.B. *et al.* (2012) Targeting glucose metabolism for cancer therapy. *J. Exp. Med.*, 209, 211–215.
2. Mindnich, R.D. *et al.* (2009) Aldo-keto reductase (AKR) superfamily: genomics and annotation. *Hum. Genomics*, 3, 362–370.
3. Chen, W.D. *et al.* (2012) Regulation of aldo-keto reductases in human diseases. *Front. Pharmacol.*, 3, 35.
4. Chung, Y.T. *et al.* (2012) Overexpression and oncogenic function of aldo-keto reductase family 1B10 (AKR1B10) in pancreatic carcinoma. *Mod. Pathol.*, 25, 758–766.
5. Matsunaga, T. *et al.* (2012) Aldo-keto reductase 1B10 and its role in proliferation capacity of drug-resistant cancers. *Front. Pharmacol.*, 3, 5.
6. Penning, T.M. (2015) The aldo-keto reductases (AKRs): overview. *Chem. Biol. Interact.*, 234, 236–246.
7. Tammali, R. *et al.* (2011) Targeting aldose reductase for the treatment of cancer. *Curr. Cancer Drug Targets*, 11, 560–571.
8. Taskoparan, B. *et al.* (2017) Opposing roles of the aldo-keto reductases AKR1B1 and AKR1B10 in colorectal cancer. *Cell. Oncol. (Dordr).*, 40, 563–578.
9. Massagué, J. *et al.* (2016) Metastatic colonization by circulating tumour cells. *Nature*, 529, 298–306.
10. Revenco, T. *et al.* (2019) Context dependency of epithelial-to-mesenchymal transition for metastasis. *Cell Rep.*, 29, 1458–1468.e3.
11. Aiello, N.M. *et al.* (2019) Context-dependent EMT programs in cancer metastasis. *J. Exp. Med.*, 216, 1016–1026.
12. Elzagheid, A. *et al.* (2012) Loss of E-cadherin expression predicts disease recurrence and shorter survival in colorectal carcinoma. *APMIS*, 120, 539–548.
13. Shioiri, M. *et al.* (2006) Slug expression is an independent prognostic parameter for poor survival in colorectal carcinoma patients. *Br. J. Cancer*, 94, 1816–1822.
14. Toiyama, Y. *et al.* (2013) Increased expression of Slug and Vimentin as novel predictive biomarkers for lymph node metastasis and poor prognosis in colorectal cancer. *Carcinogenesis*, 34, 2548–2557.
15. Schwab, A. *et al.* (2018) Polyol pathway links glucose metabolism to the aggressiveness of cancer cells. *Cancer Res.*, 78, 1604–1618.
16. Ohashi, T. *et al.* (2013) AKR1B10, a transcriptional target of p53, is downregulated in colorectal cancers associated with poor prognosis. *Mol. Cancer Res.*, 11, 1554–1563.
17. Marisa, L. *et al.* (2013) Gene expression classification of colon cancer into molecular subtypes: characterization, validation, and prognostic value. *PLoS Med.*, 10, e1001453.
18. Smith, J.J. *et al.* (2010) Experimentally derived metastasis gene expression profile predicts recurrence and death in patients with colon cancer. *Gastroenterology*, 138, 958–968.
19. Williams, C.S. *et al.* (2015) ERBB4 is over-expressed in human colon cancer and enhances cellular transformation. *Carcinogenesis*, 36, 710–718.
20. Mounir, M. *et al.* (2019) New functionalities in the TCGAbiolinks package for the study and integration of cancer data from GDC and GTEx. *PLoS Comput. Biol.*, 15, e1006701.
21. Love, M.I. *et al.* (2014) Moderated estimation of fold change and dispersion for RNA-seq data with DESeq2. *Genome Biol.*, 15, 550.
22. Demirkol, S. *et al.* (2017) A combined ULBP2 and SEMA5A expression signature as a prognostic and predictive biomarker for colon cancer. *J. Cancer*, 8, 1113–1122.
23. Demirkol, S. (2018) *Prediction of Prognosis and Chemosensitivity in Gastrointestinal Cancers*. Bilkent University. Available from: http://repository.bilkent.edu.tr/handle/11693/35716 (10 January 2019, date last accessed).
24. O'Farrell, A.C. *et al.* (2019) Implementing reverse phase protein array profiling as a sensitive method for the early pre-clinical detection of off-target toxicities associated with sunitinib malate. *Proteomics – Clin. Appl.*, 13, e1800159.
25. Predki, P.F. (2007) *Functional Protein Microarrays in Drug Discovery*. CRC Press, Boca Raton FL, USA.
26. Hu, J. *et al.* (2007) Non-parametric quantification of protein lysate arrays. *Bioinformatics*, 23, 1986–1994.
27. Young, L. *et al.* (2010) Detection of Mycoplasma in cell cultures. *Nat. Protoc.*, 5, 929–934.
28. Guan, B. *et al.* (2011) ARID1A, a factor that promotes formation of SWI/SNF-mediated chromatin remodeling, is a tumor suppressor in gynecologic cancers. *Cancer Res.*, 71, 6718–6727.
29. Pfaffl, M.W. (2001) A new mathematical model for relative quantification in real-time RT-PCR. *Nucleic Acids Res.*, 29, e45.
30. O'Connell, M.J. *et al.* (2010) Relationship between tumor gene expression and recurrence in four independent studies of patients with stage II/III colon cancer treated with surgery alone or surgery plus adjuvant fluorouracil plus leucovorin. *J. Clin. Oncol.*, 28, 3937–3944.
31. Guinney, J. *et al.* (2015) The consensus molecular subtypes of colorectal cancer. *Nat. Med.*, 21, 1350–1356.
32. Yu, G. *et al.* (2012) clusterProfiler: an R package for comparing biological themes among gene clusters. *OMICS*, 16, 284–287.
33. Ward, P.S. *et al.* (2012) Signaling in control of cell growth and metabolism. *Cold Spring Harb. Perspect. Biol.*, 4, a006783.
34. Tavares, M.R. *et al.* (2015) The S6K protein family in health and disease. *Life Sci.*, 131, 1–10.
35. Ghandi, M. *et al.* (2019) Next-generation characterization of the Cancer Cell Line Encyclopedia. *Nature*, 569, 503–508.
36. Beretta, G.D. *et al.* (2004) Adjuvant treatment of colorectal cancer. *Surg. Oncol.*, 13, 63–73.
37. Sanz-Pamplona, R. *et al.* (2012) Clinical value of prognosis gene expression signatures in colorectal cancer: a systematic review. *PLoS One*, 7, e48877.
38. Dai, G.P. *et al.* (2020) Identification of key genes for predicting colorectal cancer prognosis by integrated bioinformatics analysis. *Oncol. Lett.*, 19, 388–398.
39. Popat, S. *et al.* (2005) Systematic review of microsatellite instability and colorectal cancer prognosis. *J. Clin. Oncol.*, 23, 609–618.
40. Manning, B.D. (2004) Balancing Akt with S6K: implications for both metabolic diseases and tumorigenesis. *J. Cell Biol.*, 167, 399–403.
41. Pon, Y.L. *et al.* (2008) p70 S6 kinase promotes epithelial to mesenchymal transition through snail induction in ovarian cancer cells. *Cancer Res.*, 68, 6524–6532.
42. Magnuson, B. *et al.* (2012) Regulation and function of ribosomal protein S6 kinase (S6K) within mTOR signalling networks. *Biochem. J.*, 441, 1–21.
43. Dorrello, N.V. *et al.* (2006) S6K1- and betaTRCP-mediated degradation of PDCD4 promotes protein translation and cell growth. *Science*, 314, 467–471.
44. Mudduluru, G. *et al.* (2007) Loss of programmed cell death 4 expression marks adenoma-carcinoma transition, correlates inversely with phosphorylated protein kinase B, and is an independent

prognostic factor in resected colorectal cancer. *Cancer,* 110, 1697–1707.
45. Leupold, J.H. *et al.* (2007) Tumor suppressor Pdcd4 inhibits invasion/intravasation and regulates urokinase receptor (u-PAR) gene expression via Sp-transcription factors. *Oncogene,* 26, 4550–4562.
46. Saxena, A. *et al.* (2013) Aldose reductase inhibition suppresses colon cancer cell viability by modulating microRNA-21 mediated programmed cell death 4 (PDCD4) expression. *Eur. J. Cancer,* 49, 3311–3319.
47. Beurel, E. *et al.* (2015) Glycogen synthase kinase-3 (GSK3): regulation, actions, and diseases. *Pharmacol. Ther.,* 148, 114–131.
48. Eldar-Finkelman, H. *et al.* (1997) Phosphorylation of insulin receptor substrate 1 by glycogen synthase kinase 3 impairs insulin action. *Proc. Natl. Acad. Sci. USA*, 94, 9660–9664.
49. Ramana, K.V. (2011) Aldose reductase: new insights for an old enzyme. *Biomol. Concepts,* 2, 103–114.
50. Miyamoto, Y. *et al.* (2016) Molecular pathways: cachexia signaling-a targeted approach to cancer treatment. *Clin. Cancer Res.,* 22, 3999–4004.
51. Rommel, C. *et al.* (2001) Mediation of IGF-1-induced skeletal myotube hypertrophy by PI(3)K/Akt/mTOR and PI(3)K/Akt/GSK3 pathways. *Nat. Cell Biol.,* 3, 1009–1013.
52. Májeková, M. (2018) Ligand-based drug design of novel aldose reductase inhibitors. *Future Med. Chem.,* 10, 2493–2496.